J|A|C|S ARTICLES

Published on Web 07/15/2009

Charge Density-Dependent Modifications of Hydration Shell Waters by Hofmeister Ions

Feng Guo and Joel M. Friedman*

Department of Biophysics and Physiology, Albert Einstein College of Medicine, 1300 Morris Park Avenue, Bronx, New York 10461

Received March 29, 2009; E-mail: jfriedma@aecom.yu.edu

Abstract: Gadolinium (Gd^{3+}) vibronic sideband luminescence spectroscopy (GVSBLS) is used to probe, as a function of added Hofmeister series salts, changes in the OH stretching frequency derived from first-shell waters of aqueous Gd^{3+} and of Gd^{3+} coordinated to three different types of molecules: (i) a chelate (EDTA), (ii) structured peptides (mSE3/SE2) of the lanthanide-binding tags (LBTs) family with a single high-affinity binding site, and (iii) a calcium-binding protein (calmodulin) with four binding sites. The vibronic sideband (VSB) corresponding to the OH stretching mode of waters coordinated to Gd^{3+}, whose frequency is inversely correlated with the strength of the hydrogen bonding to neighboring waters, exhibits an increase in frequency when Gd^{3+} becomes coordinated to either EDTA, calmodulin, or mSE3 peptide. In all of these cases, the addition of cation chloride or acetate salts to the solution increases the frequency of the vibronic band originating from the OH stretching mode of the coordinated waters in a cation- and concentration-dependent fashion. The cation dependence of the frequency increase scales with charge density of the cations, giving rise to an ordering consistent with the Hofmeister ordering. On the other hand, water Raman spectroscopy shows no significant change upon addition of these salts. Additionally, it is shown that the cation effect is modulated by the specific anion used. The results indicate a mechanism of action for Hofmeister series ions in which hydrogen bonding among hydration shell waters is modulated by several factors. High charge density cations sequester waters in a configuration that precludes strong hydrogen bonding to neighboring waters. Under such conditions, anion effects emerge as anions compete for hydrogen-bonding sites with the remaining free waters on the surface of the hydration shell. The magnitude of the anion effect is both cation and Gd^{3+}-binding site specific.

Introduction

Proteins are not only a category of essential versatile biological macromolecule but also a class of polymeric molecules with significant biomedical and biotechnical potential. In order both to understand protein function *in vivo* and to harness their potential application as biomaterials, a molecular-level understanding of how external and environmental factors influence the stability, dynamics, and functionality of proteins is required. Osmolytes influence protein stability and reactivity both *in vivo* and *in vitro*. Hofmeister noted that cation and anion osmolytes can be ordered on the basis of their effect on the solubility of proteins.[1] The so-called Hofmeister series ordering has been further extended to include the effect of ions on a wide range of solution properties.[2] Since its initial description, there have been considerable interests and activities directed at exposing the underlying mechanism behind the Hofmeister series ordering of ion-specific effects; nevertheless, the origin of this ordering remains uncertain and controversial.[3,4]

One of the proposed mechanisms for the Hofmeister ordering is through ion-specific alterations in the hydrogen-bonding network of water.[2,5,6] According to whether the ions are strongly hydrated or weakly hydrated, ions have been classified as either kosmotropes (structure makers) or chaotropes (structure breakers), respectively.[2,5−7] Though supported by indirect thermodynamic and macroscopic experiments,[2,6−16] the prevailing mechanism based on ion-induced alterations in water interactions has been re-evaluated and challenged in recent studies[3,4] that indicate a lack of direct effect of ions on bulk water.[17−22]

(1) Hofmeister, F. *Arch. Exp. Pathol. Pharmakol.* **1888**, *24*, 247–260.
(2) Collins, K. D.; Washabaugh, M. W. *Q. Rev. Biophys.* **1985**, *18*, 323–422.
(3) Zhang, Y.; Cremer, P. S. *Curr. Opin. Chem. Biol.* **2006**, *10*, 658–663.
(4) Wilson, E. K. *Chem. Eng. News* **2007**, *85* (48), 47–49.
(5) Cacace, M. G.; Landau, E. M.; Ramsden, J. J. *Q. Rev. Biophys.* **1997**, *30*, 241–277.
(6) Leberman, R.; Soper, A. K. *Nature* **1995**, *378*, 364–366.
(7) Collins, K. D. *Biophys. J.* **1997**, *72*, 65–76.
(8) Robinson, R. A., Stockes, R. H. *Electrolyte Solutions*; Butterworth Scientific Publications: London, 1959.
(9) Breslow, R.; Guo, T. *Proc. Natl. Acad. Sci. U.S.A.* **1990**, *87*, 167–169.
(10) Kunz, W.; Belloni, L.; Bernard, O.; Ninham, B. W. *J. Phys. Chem. B* **2004**, *108*, 2398–2404.
(11) Ohtaki, H.; Radnai, T. *Chem. Rev.* **1993**, *93*, 1157–1204.
(12) Dillon, S. R.; Dougherty, R. C. *J. Phys. Chem. A* **2002**, *106*, 7647–7650.
(13) Nickolov, Z. S.; Miller, J. D. *J. Colloid Interface Sci.* **2005**, *287*, 572–580.
(14) Yamaguchi, T.; Lindqvist, O.; Claeson, T.; Boyce, J. B. *Chem. Phys. Lett.* **1982**, *93*, 528–532.
(15) Yamaguchi, T.; Niihara, M.; Takamuku, T.; Wakita, H.; Kanno, H. *Chem. Phys. Lett.* **1997**, *274*, 485–490.
(16) Cappa, C. D.; Smith, J. D.; Messer, B. M.; Cohen, R. C.; Saykally, R. J. *J. Phys. Chem. B* **2006**, *110*, 5301–5309.

10.1021/ja902240j CCC: $40.75

Molecular simulation studies have provided contradictory descriptions based on chosen models and initial parameters.[22−24]

A possible reconciliation among these two different views and sets of results relating to the origin of the Hofmeister series might emerge from recent findings that ions accumulate and perturb local water structure at surface interfaces, including protein/water interfaces. The degree of ion accumulation appears to scale with their ordering within the Hofmeister series.[3,25] It is in this critical interface between macromolecules such as proteins and the bulk solvent that one finds hydration shell waters. It is becoming ever more apparent that protein stability, dynamics, and function are directly tied to hydration shell properties.[26−31] Thus, potentially, ions that alter the hydration layer surrounding a protein can impact protein properties without significant perturbation on water interactions in the bulk solvent regime.

The recent studies that have led to a revision in thinking regarding the origin of the Hofmeister ordering have all focused on Hofmeister anions because of their large ionic radii and close distance to water molecules. In contrast, the present study focuses on the interplay between Hofmeister cations and anions and how this interplay is modulated by specific environments. The conceptual framework for analyzing the data is based on a simplistic model in which water structure is inhomogeneous on a nanoscopic level and water properties result from perturbations influencing the balance between two interconverting microstructural components of water: high-density clusters and low-density clusters.[32−44] In this scheme, the difference in the properties between the two clusters arises largely from hydrogen bonding among waters within the high-density clusters being weaker than in the low-density clusters. It has also been proposed that distinctions between bulk and hydration water layers originate from a different fractional composition of two types of water clusters within these two solvent regimes.[36]

The effect of added salts on water interactions is probed using a novel spectroscopic technique that provides the vibrational frequencies of waters in the hydration shell of Gd^{3+}. The Gd^{3+} cation is an especially suitable probe in that it readily replaces the similarly sized Ca^{2+} in chelates and calcium-binding sites in proteins and peptides without disruption of the native structure.[45−48] The technique allows for probing of how a series of added Hofmeister salts influence hydrogen bonding among hydration waters both for the free Gd^{3+} in solution and for Gd^{3+} coordinated to a series of biologically relevant calcium-binding sites.

The specificity and utility of this technique are based on earlier findings that Gd^{3+} vibronic sideband luminescence spectroscopy (GVSBLS) can provide an infrared-like vibrational spectrum derived exclusively from molecules surrounding Gd^{3+}, including those of coordinated first-shell waters.[49−51] Changes in the vibrational frequencies from the first-shell water molecule reflect changes in their hydrogen bonding to outer-sphere solvent molecules.[52−54] As such, GVSBLS is a potent molecular-level probe of hydrogen bonding within the hydration shell of Gd^{3+}. GVSBLS is derived from the Gd^{3+} luminescence spectrum in which there are weak vibronic (vibration plus electronic) side bands (VSBs) associated with pure electronic transition from the lowest excited electronic state to the ground electronic state[50,55] (Figure 1). These VSBs correspond to transitions which couple a change in both the electronic state of the Gd^{3+} and the vibrational state of nearby molecules. Figure 1a,c shows that the ∼273 nm (36 630 cm^{-1}) excited luminescence spectrum of Gd^{3+} in pure aqueous solution arises overwhelmingly from a single electronic transition, $^6P_{7/2} \rightarrow {}^6S_{7/2}$, at ∼311 nm (32 154 cm^{-1}). The separation in frequencies between the electronic and the vibronic transitions yields the energy of the vibrational transition for molecular species in the immediate environment of Gd^{3+} (Figure 1b). GVSBLS technique has been successfully used to probe the Gd^{3+}-associated ligands when the Gd^{3+} cation is coordinated to calcium-binding proteins, phospholipids, and

(17) Omta, A. W.; Kropman, M. F.; Woutersen, S.; Bakker, H. J. *Science* **2003**, *301*, 347–349.
(18) Kropman, M. F.; Bakker, H. J. *Science* **2001**, *291*, 2118–2120.
(19) Batchelor, J. D.; Olteanu, A.; Tripathy, A.; Pielak, G. J. *J. Am. Chem. Soc.* **2004**, *126*, 1958–1961.
(20) Naslund, L. A.; Edwards, D. C.; Wernet, P.; Bergmann, U.; Ogasawara, H.; Pettersson, L. G. M.; Myneni, S.; Nilsson, A. *J. Phys. Chem. A* **2005**, *109*, 5995–6002.
(21) Bakker, H. J.; Kropman, M. F.; Omta, A. W. *J. Phys.: Condensed Matter* **2005**, *17*, S3215.
(22) Smith, J. D.; Saykally, R. J.; Geissler, P. L. *J. Am. Chem. Soc.* **2007**, *129*, 13847–13856.
(23) Hribar, B.; Southall, N. T.; Vlachy, V.; Dill, K. A. *J. Am. Chem. Soc.* **2002**, *124*, 12302–12311.
(24) Thomas, A. S.; Elcock, A. H. *J. Am. Chem. Soc.* **2007**, *129*, 14887–14898.
(25) Chen, X.; Yang, T.; Kataoka, S.; Cremer, P. S. *J. Am. Chem. Soc.* **2007**, *129*, 12272–12279.
(26) Frauenfelder, H.; McMahon, B. H.; Fenimore, P. W. *Proc. Natl. Acad. Sci. U.S.A.* **2003**, *100*, 8615–8617.
(27) Fenimore, P. W.; Frauenfelder, H.; McMahon, B. H.; Parak, F. G. *Proc. Natl. Acad. Sci. U.S.A.* **2002**, *99*, 16047–16051.
(28) Frauenfelder, H.; Fenimore, P. W.; Chen, G.; McMahon, B. H. *Proc. Natl. Acad. Sci. U.S.A.* **2006**, *103*, 15469–15472.
(29) Samuni, U.; Dantsker, D.; Roche, C. J.; Friedman, J. M. *Gene* **2007**, *398*, 234–248.
(30) Samuni, U.; Roche, C. J.; Dantsker, D.; Friedman, J. M. *J. Am. Chem. Soc.* **2007**, *129*, 12756–12764.
(31) Henzler-Wildman, K. A.; Lei, M.; Thai, V.; Kerns, S. J.; Karplus, M.; Kern, D. *Nature* **2007**, *450*, 913–916.
(32) Vedamuthu, M.; Singh, S.; Robinson, G. W. *J. Phys. Chem.* **1994**, *98*, 2222–2230.
(33) Sudhakar, K.; Phillips, C. M.; Owen, C. S.; Vanderkooi, J. M. *Biochemistry* **1995**, *34*, 1355–1363.
(34) Hepler, L. G. *Can. J. Chem.* **1969**, *47*, 4613–4617.
(35) Lin, L.-N.; Brandts, J. F.; Brandts, J. M.; Plotnikov, V. *Anal. Biochem.* **2002**, *302*, 144–160.
(36) Chalikian, T. V. *J. Phys. Chem. B* **2001**, *105*, 12566–12578.
(37) Head-Gordon, T.; Hura, G. *Chem. Rev.* **2002**, *102*, 2651–2670.
(38) Vogler, E. A. *Adv. Colloid Interface Sci.* **1998**, *74*, 69–117.
(39) Robinson, G. W.; Cho, C. H.; Urquidi, J. *J. Chem. Phys.* **1999**, *111*, 698–702.
(40) Cho, C. H.; Urquidi, J.; Gellene, G. I.; Robinson, G. W. *J. Chem. Phys.* **2001**, *114*, 3157–3162.
(41) Cho, C. H.; Urquidi, J.; Gellene, G. I. *J. Chem. Phys.* **2001**, *115*, 7796–7797.
(42) Cho, C. H.; Urquidi, J.; Robinson, G. W. *J. Chem. Phys.* **1999**, *111*, 10171–10176.
(43) Robinson, G. W.; Cho, C. H. *Biophys. J.* **1999**, *77*, 3311–3318.
(44) Kotera, K.; Saito, T.; Yamanaka, T. *Phys. Lett. A* **2005**, *345*, 184–190.
(45) Birnbaum, E. R.; Gomez, J. E.; Darnall, D. W. *J. Am. Chem. Soc.* **1970**, *92*, 5287–5288.
(46) Martin, R. B.; Richardson, F. S. *Q. Rev. Biophys.* **1979**, *12*, 181–209.
(47) Smolka, G. E.; Birnbaum, E. R.; Darnall, D. W. *Biochemistry* **1971**, *10*, 4556–4561.
(48) Darnall, D. W.; Birnbaum, E. R. *J. Biol. Chem.* **1970**, *245*, 6484–6486.
(49) Haas, Y.; Stein, G. *Chem. Phys. Lett.* **1971**, *11*, 143–145.
(50) Stavola, M.; Friedman, J. M.; Stepnoski, R. A.; Sceats, M. G. *Chem. Phys. Lett.* **1981**, *80*, 192–194.
(51) Iben, I. E.; Stavola, M.; Macgregor, R. B.; Zhang, X. Y.; Friedman, J. M. *Biophys. J.* **1991**, *59*, 1040–1049.
(52) Jeffrey, G. A. *An introdduction to hydrogen bonding*; Oxford University Press: New York, 1997.
(53) Pimental, G. C.; McClellan, A. L. *The Hydrogen Bond*; W.H. Freeman and Co.: San Francisco/London, 1960.
(54) Vanderkooi, J. M.; Dashnau, J. L.; Zelent, B. *Biochim. Biophys. Acta* **2005**, *1749*, 214–233.
(55) Freed, S. *Rev. Mod. Phys.* **1942**, *14*, 105–111.

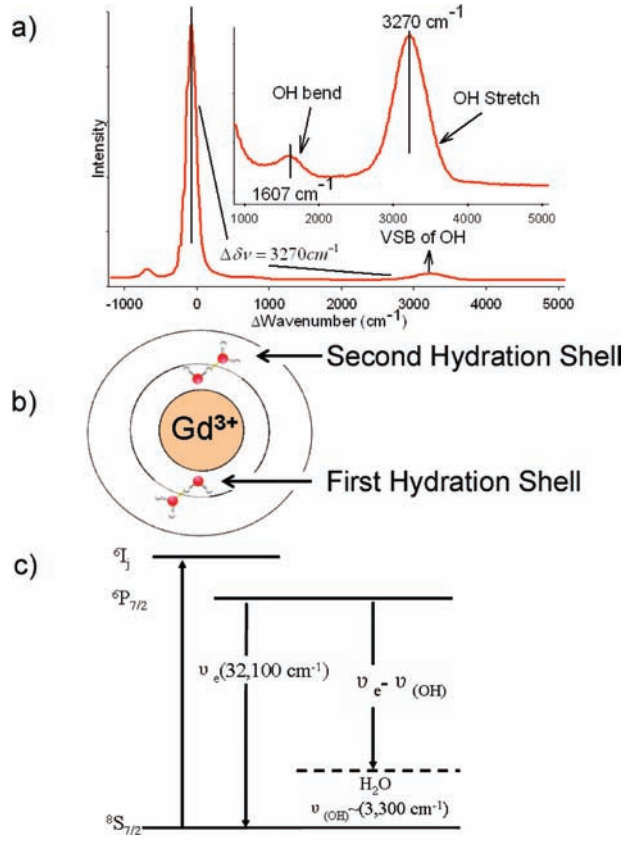

Figure 1. (a) Luminescence spectrum of 1 M aqueous gadolinium solution, showing the vibronic side bands (VSBs) originating from the water bending and OH stretching modes of waters in the first hydration shell of the Gd^{3+}. The excitation wavelength was 273 nm. *X*-axis is calibrated to represent the energy difference from the pure electronic transition centered at 311 nm (32 154 cm^{-1}). (b) Diagram showing the first and second hydration shell waters surrounding Gd^{3+}. The OH stretch frequency is inversely correlated with the strength of the hydrogen bond to the second-layer water. Therefore, the OH stretching frequency monitored in the VSB spectrum is a specific probe of the local hydrogen bonding in the hydration shell of Gd^{3+}. (c) Simplified energy level diagram of hydrated Gd^{3+}.

DNA[51] as well as alcohols, crown ethers, carbonate, phosphate, and several other assorted organic molecules.[56] The technique has also been applied to probe the waters within porous sol−gels and glasses.[57]

In the present study, changes in the O−H stretching frequencies from the first-shell waters of the Gd^{3+} cation are monitored as a function of added salts. This frequency is inversely correlated with the strength of the hydrogen bonding to second-shell waters. Thus, through VSBLS, the water coordinated to the Gd^{3+} cation becomes a probe of how added salts perturb hydrogen bonding between the "probe" waters on the surface of the Gd^{3+} cation and those in the adjacent layer. This approach is applied to aqueous hydrated Gd^{3+} and to Gd^{3+} coordinated to three different binding environments: EDTA, calmodulin,[58] and peptides from an optimally developed family of molecularly engineered lanthanide-binding tags (LBTs).[59−63] In most instances, the chloride and acetate salts of the tested cations are used to eliminate effects due to different anions when comparing different cations. Additionally, different halide salts of magnesium, potassium, and sodium are compared to evaluate the anion specificity of the cation effect.

All of these Gd^{3+}-binding molecules have well-characterized calcium-binding sites. There are three or four coordinated water molecules in the single binding site of Gd^{3+}-coordinated EDTA that are hydrogen bonded to the waters in the outer hydration shell.[51,64,65] Calmodulin[63] has four binding sites, of which I and II have similar higher affinity for Gd^{3+}. In each of the higher affinity binding sites, one water is found coordinated to the bound metal ions.[66] The complexity due to the mixed stretch frequency behaviors of either the multiple first hydration waters of coordinated Gd^{3+} in EDTA or the single first hydration water from multiple binding sites in calmodulin is addressed by employing 17 amino acid LBT peptides that have a single EF hand calcium-binding motif similar to those seen in typical calcium-binding proteins such as troponin c.[59−61] Relatively modest site-specific changes in a troponin c-based EF hand motif have produced LBTs with extremely high affinity for lanthanides.[59−61] Two LBTs are chosen: mSE3 that has single water coordinated to a bound lanthanide, and SE2 with no water in the inner hydration sphere of the coordinated lanthanide[59−61] (also supported by unpublished results from Langdon Martin in the B. Imperiali laboratory at MIT; see Supplemental Table 1 in the Supporting Information for the amino acid sequences of mSE3 and SE2). The single coordinated water in mSE3 allows for a more straightforward comparison of the effect of added Hofmeister cations on the hydrogen bonding between the first-shell water of the bound lanthanide ion and adjacent waters.

The results show a clear pattern in which, for chloride or acetate anions, added cations weaken the hydrogen bond between the first- and second-shell waters, and the degree of weakening follows ordering consistent with both the Hofmeister series and the charge density of cations.

Experimental Section

SE2 and mSE3 peptides were obtained as a generous gift from Dr. Barbara Imperiali (Department of Chemistry, Massachusetts Institute of Technology). All other materials were purchased from Aldrich-Sigma and used without further purification. Calmodulin from bovine testes was purchased as BioUltra grade.

All aqueous samples were prepared using distilled deionized water. Aqueous unbound $GdCl_3$ samples for titration of Hofmeister series salts were made by mixing $GdCl_3$ stock solution with suitable aliquots of salt stock solutions to achieve a final concentration of 0.5 M $GdCl_3$ with the desired amount of salts.

Solutions of 100 mM EDTA, 1 mM calmodulin, and 1 mM apo-mSE3 and 1 mM apo-SE2 were prepared in 10 mM HEPES buffer at pH 7.0 with 80 mM, 1 mM, and 1 mM $GdCl_3$, respectively. The extremely high affinity of Gd^{3+} for all of the binding sites in these calcium-binding materials ensures that, under the experimental conditions, all the Gd^{3+} coordinates to the binding sites at the

(56) MacGregor, R. B., Jr. *Arch. Biochem. Biophys.* **1989**, *274*, 312–316.
(57) Navati, M. S.; Ray, A.; Shamir, J.; Friedman, J. M. *J. Phys. Chem. B* **2004**, *108*, 1321–1327.
(58) Wallace, R. W.; Tallant, E. A.; Cheung, W. Y. *Cold Spring Harbor Symp. Quant. Biol.* **1982**, *46* (Pt. 2), 893–901.
(59) Franz, K. J.; Nitz, M.; Imperiali, B. *ChemBioChem* **2003**, *4*, 265–271.
(60) Nitz, M.; Franz, K. J.; Maglathlin, R. L.; Imperiali, B. *ChemBioChem* **2003**, *4*, 272–276.
(61) Nitz, M.; Sherawat, M.; Franz, K. J.; Peisach, E.; Allen, K. N.; Imperiali, B. *Angew. Chem., Int. Ed.* **2004**, *43*, 3682–3685.
(62) Lim, S.; Franklin, S. J. *Cell. Mol. Life Sci.* **2004**, *61*, 2184–2188.
(63) Snyder, E. E.; Buoscio, B. W.; Falke, J. J. *Biochemistry* **1990**, *29*, 3937–4943.
(64) Horrocks, W. D. J.; Sudnick, D. R. *Acc. Chem. Res.* **1981**, *14*, 384–392.
(65) Gschneidner, K. A.; Eyring L. R. *The Handbook on the Physics and Chemistry of Rare Earths.*; North-Holland Publishing Co.: Amsterdam, 1979; Vol. 3.
(66) Chattopadhyaya, R.; Meador, W. E.; Means, A. R.; Quiocho, F. A. *J. Mol. Biol.* **1992**, *228*, 1177–1192.

concentrations used (see Supplemental Table 2 in the Supporting Information for detailed binding constants). Aliquots of salt stock solutions were added to these samples to compare ion-specific effects on the hydration shell waters of coordinated Gd^{3+}. The relatively weak affinity of added cations other than Gd^{3+} prevents the substitution of coordinated Gd^{3+} with Hofmeister series cations used in the present studies (see Supplemental Table 2). Trehalose-derived glass matrices doped with $GdCl_3$ and salts were prepared by dissolving 0.25 M $GdCl_3$ and 0.5 M salts with 100 mg of trehalose in 1 mL solution. Aliquots of the solution were placed on the horizontally positioned surface of glass sheets and dried under a vacuum in a desiccator until a transparent glass film was formed. The glass films were put in an oven at 50 °C for 1 h for further drying.

The Raman spectrum of the OH stretching mode of bulk water and the GVSBLS were acquired on a QuantaMaster model QM-4/2000SE enhanced performance scanning spectrofluorometer (Photon Technology International, Lawrenceville, NJ). All of the solution samples were contained in quartz cuvettes and probed using 90° excitation geometry, while glass samples were probed using front face geometry (around 45°). The Raman spectra were generated using a 350 nm excitation. For GVSBLS the excitation wavelength was around 273 nm, where Gd^{3+} has a relatively enhanced absorption cross section. Continuous-wave excitation to generate GVSBLS was used for samples of unbound Gd^{3+} and of Gd^{3+}-coordinated EDTA. Time-gated GVSBLS was used for Gd^{3+}-coordinated calmodulin and mSE3/SE2 samples to eliminate short-lived fluorescence signals from the protein or peptides (see Supplemental Figure 1 in the Supporting Information). The gated GVSBLS were accumulated from a time point starting from 100 μs through 1000 μs after the pulsed excitation source. The luminescence spectrum was scanned and recorded from 290 to 400 nm. To rule out the possibility that the observed weak signals were not due to Raman scattering (for the ungated signals) or non-Gd^{3+}-derived fluorescence, excitation profiles were routinely obtained for observed peaks in emission spectra. The emission monochromator slits were adjusted in order to obtain suitable signal-to-noise ratios. The luminescence spectra were plotted as intensity vs frequency shift (cm^{-1}) from the electronic peak at 311 nm (32 154 cm^{-1}) to represent the energy difference that is equal to the vibration frequency of coordinated ligands. The spectra were processed and analyzed using GRAMS/32 AI (6.00) for background subtraction, smoothing, and peak analysis.

The accuracy of the high-resolution fluorometer achieves ±0.1 nm, which equals ±8 cm^{-1} in the region of the vibronic sideband upon converting spectra from wavelength (nm) to wavenumber (cm^{-1}). [Calculation: $\Delta\nu(cm^{-1}) = 10^7(\Delta\lambda(nm)/\lambda_1\lambda_2)$. The vibronic sideband is around 346 nm. Therefore, $\Delta\lambda = \pm 0.1$ nm, $\lambda_1 \approx \lambda_2 =$ 346 nm, and $\Delta\nu \approx \pm 8$ cm^{-1}.] Another factor contributing to uncertainty in the peak position assignment is the random error that arises from the difference from one trace to the next, which can be controlled by averaging multiple repeated traces. The number of averaged traces is based on the signal-to-noise ratio associated with the individual trace. For protein-free samples where the signal-to-noise ratio is very high, an average of three traces is typical, whereas for samples with weak signals, averaging can consist of as many as 100 scans. Ordering of small peak shifts is verified by directly overlapping the normalized average spectra and comparing vibronic bands from samples with different additives. The intense electronic band at ~311 nm, which does not shift under these conditions, serves as a wavelength/frequency reference point. Under these conditions, the entire peak band profile contributes to the evaluation (as opposed to just comparing peak positions), permitting facile determination if an entire band has shifted relative to another band, given that the line shape/bandwidth does not change. It is consequently possible to detect shifts smaller than the resolution associated with a given wavelength, similarly to difference spectra analysis. The ordering with respect to which samples shift more than others is therefore still valid, even though the actual magnitude of the small shifts could be less than 10 cm^{-1}, and claims of specific shifts in excess of 10 cm^{-1} are precisely accurate. Most of the measurements have been repeated on different samples on different occasions, yielding consistent results, and the trends are very clear and do not rest upon the exact values associated with the smallest shifts or small differences among many samples. The issues are similar to those associated with many FTIR and Raman studies.

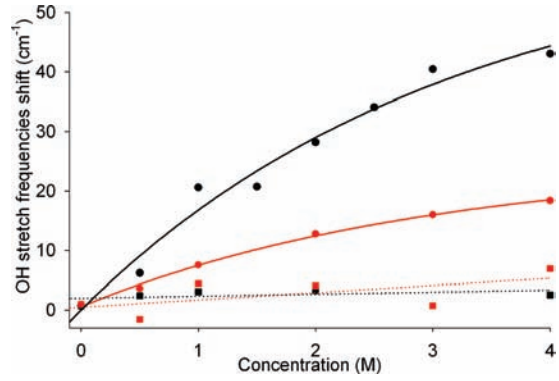

Figure 2. Plot of the frequency shift of −OH stretching mode vibration derived from (circles) GVSBLS and (squares) Raman of 0.5 M Gd^{3+} in aqueous solution with $MgCl_2$ (black) and NaCl (red).

The frequency of the VSB arising from the water stretching mode (~3300 cm^{-1}) measures hydrogen bonding between the first-shell waters and the outer group.[50,67] A decrease or increase of this frequency is correlated with an increase or decrease in hydrogen bond strength, respectively.

Results

Cation-Specific Effects on the OH Stretching Frequency of Waters in the First Hydration Shell of Free Aqueous Gd^{3+}. Figure 2 shows a plot of the increase in the frequency of the OH stretching of hydration shell waters derived from the GVSBLS of free Gd^{3+} as a function of added $MgCl_2$ and NaCl. It can be seen that with added salts the OH stretching frequency increases. At any given concentration of added salts, $MgCl_2$ is seen to be significantly more effective in causing a frequency increase than NaCl. The figure also shows that the OH stretching frequency observed in the Raman spectrum from the same samples shows essentially no change with added salts. Whereas the GVSBLS probes only those waters in the hydration shell of Gd^{3+}, the Raman probes all waters.

OH Stretching Frequency of Water in the Hydration Shell of Coordinated Gd^{3+}. Figure 3 shows the GVSBL spectra of EDTA-coordinated Gd^{3+} in the presence and in the absence of 4.0 M $MgCl_2$. In addition to the VSB corresponding to the OH stretching mode, there are several other observable bands. The intense VSBs at 1425 and 1600 cm^{-1}, which do not appear for the free aqueous Gd^{3+} sample, are the previously assigned[51] symmetric and antisymmetric stretching modes of the EDTA-derived C═O groups coordinated to bound Gd^{3+}. The small shoulder around 3000 cm^{-1} has been attributed[51] to the stretching of C−H groups in close proximity to Gd^{3+}. Similar VSBs are also observed for calmodulin (Supplemental Figure 2, Supporting Information) and mSE3 coordinated Gd^{3+} (Supplemental Figure 3, Supporting Information). Both calmodulin and the peptide manifest an OH stretching VSB. In contrast, the peptide SE2, known to not have any water coordinated to Gd^{3+}, does not manifest an OH band in the GVSBLS (data not shown).

(67) Stavola, M.; Isganitis, L.; Sceats, M. G. *J. Chem. Phys.* **1981**, *74*, 4228–4241.

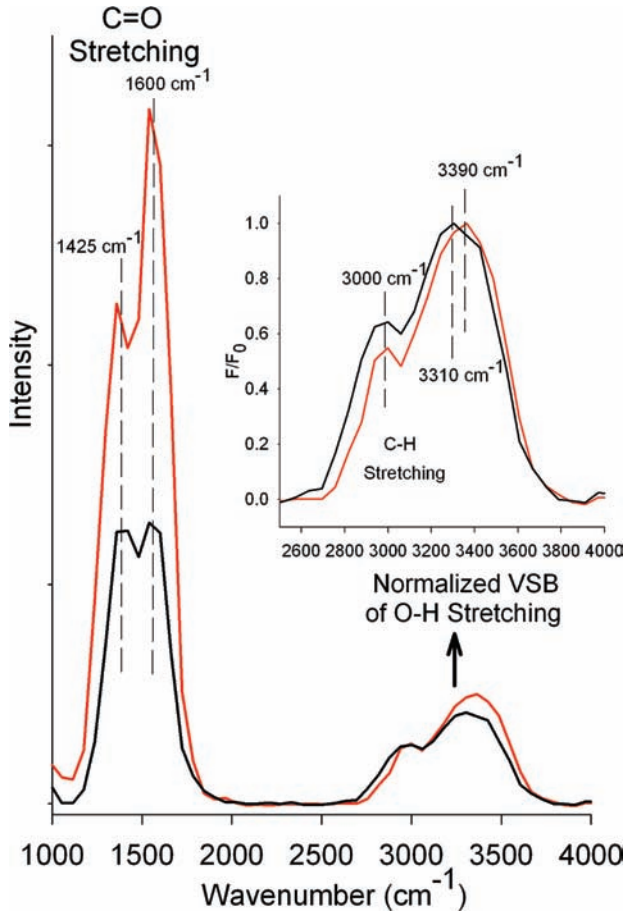

Figure 3. VSBs for samples of 100 mM EDTA and 80 mM Gd^{3+} in 10 mM HEPES buffer at pH 7.0 in the absence of $MgCl_2$ (black) and in the presence of 4.0 M $MgCl_2$ (red). Inset: Normalized −OH stretching mode VSB.

The comparison of the OH VSB spectra of free Gd^{3+} and Gd^{3+} coordinated to EDTA, calmodulin, or mSE3 reveals a similar pattern in that coordination results in an increase in the OH stretching frequency. The OH stretch frequency increases by 40, 30, and 120 cm^{-1} on going from free Gd^{3+} to EDTA-coordinated Gd^{3+}, to calmodulin-coordinated Gd^{3+}, and to mSE3-coordinated Gd^{3+}, respectively (see Supplemental Table 3 in the Supporting Information). This result is consistent with previous findings derived from parvalbumin-coordinated Gd^{3+}, where an increase in the OH stretching frequency was also observed upon coordination.[51] It is also observed that the peak bandwidth substantially increases for protein- and peptide-bound samples (see Supplemental Figures 2 and 3).

Cation-Dependent Frequency Shifts in the OH Stretching Band in the GVSBLS. Addition of $MgCl_2$ and NaCl results in a concentration-dependent increase in the frequency of the water stretching mode in the VSB spectrum from EDTA-coordinated Gd^{3+} (Figure 3), calmodulin-coordinated Gd^{3+} (Supplemental Figure 4, Supporting Information), and peptide-coordinated Gd^{3+} (Supplemental Figure 3). The pattern for the concentration and cation dependence is similar to that observed for the OH stretching VSB from free Gd^{3+} (Figure 1). In contrast to the OH stretching band, the VSB frequencies for the C═O and C−H bands do not respond to the added salts, as seen for EDTA-coordinated Gd^{3+} (Figure 3), calmodulin-coordinated Gd^{3+} (Supplemental Figure 4), and peptide-coordinated Gd^{3+} (Supplemental Figure 3).

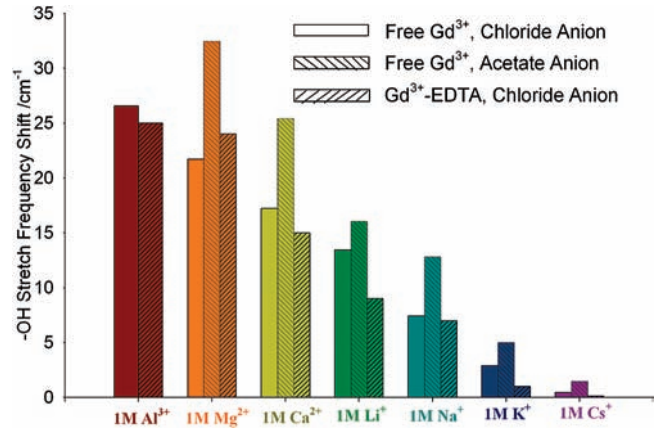

Figure 4. Bar graph of OH stretch vibration frequency shift of first hydration shell waters of 0.5 M $GdCl_3$ with chloride salts, 0.5 M $GdCl_3$ with acetate salts, and 80 mM EDTA−Gd^{3+} with chloride salts.

Figure 4 compares, for free and EDTA-coordinated Gd^{3+}, the VSB OH frequencies as a function of cation for a series of added chloride and acetate salts at the same 1.0 M concentration. The plot is ordered with respect to charge density of the added cations. It can be seen that the magnitude of the frequency increase scales with charge density of the added cation. The increase in the frequency of the OH stretching band occurs for salts with either counteranion. The frequency increase relative to the salt-free Gd^{3+} solution increases in the following order: $Cs^+ < K^+ < Na^+ < Li^+ < Ca^{2+} < Mg^{2+} < Al^{3+}$. The values for these frequencies and frequency shifts are summarized in Supplemental Table 4 in the Supporting Information. This ordering roughly matches the Hofmeister series ordering, reflected in the value of the Setchenow constant that directly indicates the relative salting-out ability of a given ion[68] (see Supplemental Figure 5 in the Supporting Information).

Figure 4 demonstrates that the cation-dependent VSB OH frequency increase as a function of added cation salts is similar for EDTA-coordinated Gd^{3+} and free Gd^{3+}. A similar pattern on a less extensive set of salts is also seen for the protein- and peptides-coordinated Gd^{3+}. Although the general patterns are similar for all of the Gd^{3+} complexes, the actual magnitude of the response to the added salts is dependent on both the particular environment of the Gd^{3+} and the specific cation, as shown in Figure 5. The values of the cation-dependent frequencies and shifts for the coordinated samples are provided in Supplemental Table 5 in the Supporting Information.

Included in Figure 5 is the frequency for $GdCl_3$ powder that has been dried for several hours. This degree of drying is associated with a VSB OH frequency that has undergone the largest increase relative to the initial unheated hydrated powder. Continued heating beyond this point resulted in a loss of the OH VSB, indicative of complete loss of first-shell hydration waters. The OH VSB band reappears when the powder is exposed to a humid atmosphere. Similarly, the initial heating-induced increase in OH frequency is attributed to a progressive loss of second-shell waters, resulting in an absence of hydrogen-bonding interactions for the first-shell waters. The similar frequencies for the OH VSB for mSE3 peptide-coordinated Gd^{3+} in the presence of 4 M $MgCl_2$ and the heated powder indicates that, under these conditions, there is very weak or no hydrogen bonding between the single first-shell water of the peptide-coordinated Gd^{3+} and surrounding waters.

(68) Baldwin, R. L. *Biophys. J.* **1996**, *71*, 2056–2063.

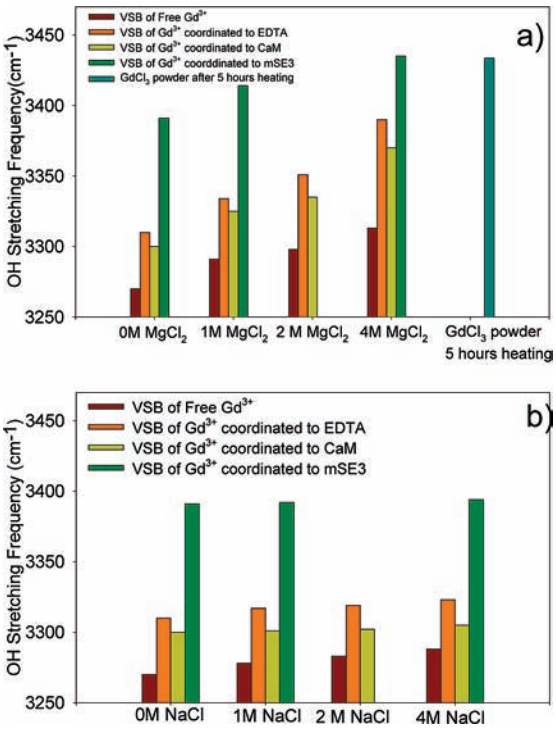

Figure 5. (a). Bar graph of −OH stretching mode vibration frequencies derived from GVSBLS as a function of added $MgCl_2$ for the following samples: (red) 0.5 M Gd^{3+}, (orange) 100 mM EDTA with 80 mM Gd^{3+} in 10 mM HEPES buffer at pH 7.0, (yellow) 1 mM calmodulin and 1 mM Gd^{3+} in 10 mM HEPES buffer at pH 7.0, and (green) 1 mM mSE3 and 1 mM Gd^{3+} in 10 mM HEPES buffer at pH 7.0. Also shown is a bar graph (blue) of −OH stretching mode vibration frequency derived from GVSBLS of hydrated $GdCl_3$ powder heated for 5 h. (b). Bar graph of −OH stretching mode vibration frequency derived from GVSBLS as a function of added NaCl for the following samples: (red) 0.5 M Gd^{3+}, (orange) 100 mM EDTA with 80 mM Gd^{3+} in 10 mM HEPES buffer at pH 7.0, (yellow) 1 mM calmodulin and 1 mM Gd^{3+} in 10 mM HEPES buffer at pH 7.0, and (green) 1 mM mSE3 and 1 mM Gd^{3+} in 10 mM HEPES buffer at pH 7.0 with varied concentration of NaCl.

Anion Specificity Associated with the Effect of Added Salts on the OH Stretching Frequency of Water in the Hydration Shell of Free Aqueous $Gd^{3+}$and Gd^{3+} Coordinated to EDTA. The above cation-specific effects were all established using chloride salts. Acetate salts added to the free Gd^{3+} yield results closely resembling those obtained with chloride as shown in Figure 4. In Figure 6a is shown the OH stretching frequency for free Gd^{3+} and EDTA-coordinated Gd^{3+} as a function of added magnesium salts. There is minimal effect due to the added fluoride salt; however, the very low solubility of this salt does not allow for a valid comparison with the two other shown magnesium salts, which are at the 1 M level. Additionally, attempts to compare the iodide salt of magnesium were also thwarted by extremely low solubility. There is slight suggestion of a frequency increase on going from the chloride to the bromide, with both salts causing a large frequency increase relative to the salt-free solution. In Figure 6b, it can be seen that none of the potassium salts are effective in significantly changing the frequency relative to the salt-free samples. There is a suggestive pattern of increasing frequencies for the following sequence of anion salts of potassium: F^-, Cl^-, Br^-, and I^-. The anion dependence is significantly more dramatic for the sodium cation, as shown in Figure 6c. It can be seen that both the fluoride actually decreases the OH stretching frequency relative to the salt-free solution and the frequency increases on going from F^- to Cl^- to Br^- to I^-. (It is the classic Hofmeister signature with a change in sign of the ion effect with the strength of water−water interactions.) Whenever an anion effect can be compared as a function of the specific cation, the effect increases on going from potassium to sodium to magnesium. Supplemental Table 6 in the Supporting Information provides the actual frequencies associated with each of these solutions.

As will be discussed in the next section, the emerging model that accounts for the change in OH stretching frequency in the hydration shell of the Gd^{3+} includes competition between free mobile waters and anions for hydrogen-bonding partners of the first-shell waters around the Gd^{3+}. The expectation is that, in an environment that reduces the population of mobile waters, there will be an exaggerated cation-dependent anion effect. Water molecules contained within dry glassy matrices derived from sugars such as trehalose are essentially sequestered by being incorporated into an extended hydrogen-bonding network. As a result, there are fewer waters available to participate in strong hydration shell interactions associated with added dopants within the glass. Under this condition, anions may become more competitive *vis à vis* water for sites in the second shell of the solvation layer. Figure 6d shows the effect of added salts on the frequency of the OH stretching mode in the vibronic spectrum of Gd^{3+} within a dry glass made from trehalose. Addition of the different salts to the Gd^{3+}-doped glass elicits a pattern that is similar to but more exaggerated than what is seen in solution. The chloride salt of sodium has a very minimal impact on the OH stretching frequency, as is seen in solution for the free Gd^{3+}. In contrast, the reduction of the OH stretching frequency seen in solution for free Gd^{3+} with the addition of NaF is duplicated in the glass but in an exaggerated fashion. Similarly, the $MgCl_2$-induced frequency increase seen in solution is also seen in the glass but with a dramatically enhanced magnitude. The shifts and frequencies are included in Supplemental Table 6.

Discussion

Salt-Induced Change in the Hydrogen Bonding within the Hydration Shell of Both Free and Coordinated Gd^{3+}. The presented results show that the addition of salts can modulate hydrogen bonding between waters in the first and second hydration layers surrounding Gd^{3+}. For a given salt, the magnitude of the effect increases with increasing concentration of the added salt. For added salts with low charge density anions such as chloride, bromide, iodide, and acetate, there is weakening effect that is a function of the specific cation. The magnitude of the weakening, as reflected in the increase in the OH stretching frequency in the vibronic spectrum, scales with the charge density of the cation for a given concentration of added salts. The higher the charge density of the cation, the greater is the weakening of the hydrogen bonding for a given anion. The overall observed pattern of anion and cation effects in this study is similar to a pattern derived from a simulation[23] in that both studies show opposite patterns for cations and anions with respect to the dependence of hydrogen bonding on charge density.

The results derived from the direct comparison of cations with triple, double, or single valence under the same salt concentration are potentially complicated because the counter-anion concentrations are significantly different. Figure 2 shows that, when comparing the Mg^{2+} and Na^+ cations under conditions of the same chloride concentration, the Mg^{2+} cation still manifests the larger effect on the OH stretching frequency. This issue was further addressed by conducting comparisons among

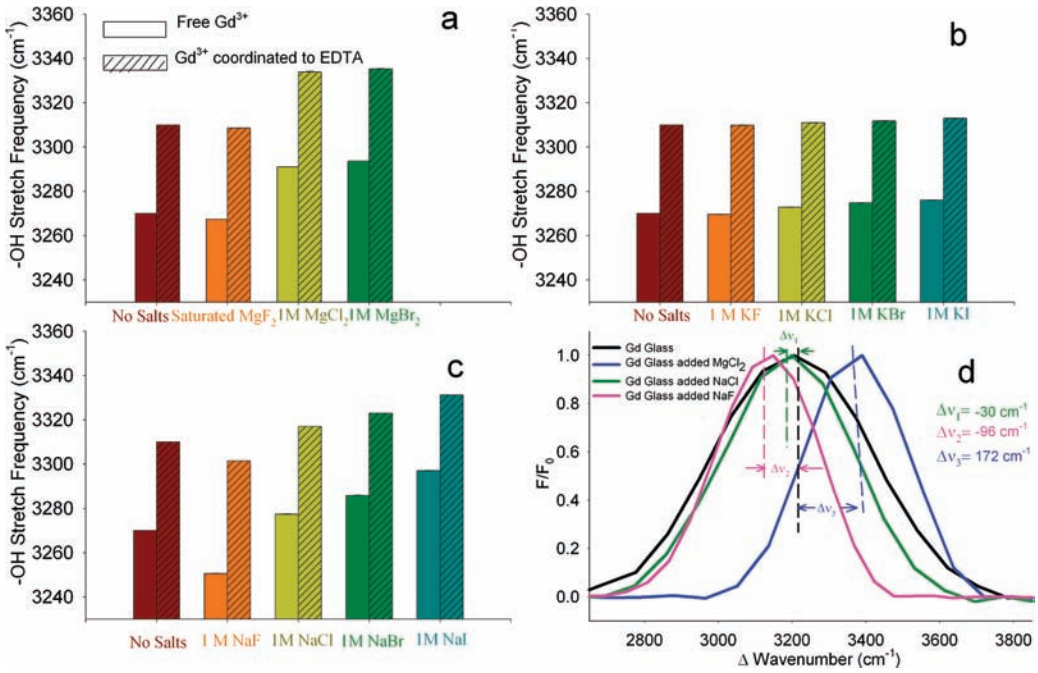

Figure 6. (a−c) Bar graphs of −OH stretching mode vibration frequency derived from GVSBLS of 0.5 M Gd^{3+} (solid bars) and 100 mM EDTA with 80 mM Gd^{3+} in 10 mM HEPES buffer at pH 7.0 (striped bars): (a) in the absence of salts (red) and in the presence of saturated MgF_2 (orange), 1 M $MgCl_2$ (yellow), and 1 M $MgBr_2$ (green); (b) in the absence of salts (red) and in the presence of 1 M KF (orange), 1 M KCl (yellow), 1 M KBr (green), and 1 M KI (blue); and (c) in the absence of salts (red) and in the presence of 1 M NaF (orange), 1 M NaCl (yellow), 1 M NaBr (green), and 1 M NaI (blue). (d) Plot of the frequency shift of −OH stretching mode vibration derived from GVSBLS of 0.25 M $GdCl_3$ in trehalose glassy matrices in the absence (black) and in the presence of $MgCl_2$ (blue), NaCl (green), and NaF (purple). The original concentration of salts is 0.5 M.

cations under the condition of high KCl concentration (4 M). The K^+ cation has little or no effect on the OH stretching frequency, and the chloride concentration is high enough to minimize differences in the chloride concentration when comparing the effects of cations at the same concentration. It is observed (Supplemental Figures 6 and 7 in the Supporting Information) that, at the high chloride concentration, the magnitude of the OH frequency shift still tracks with the charge density of the cation ($Al^{3+} > Mg^{2+} > Na^+$).

The comparison of the hydrogen bond weakening effect for the magnesium, sodium, and potassium halide salt series also indicates that, for both free and coordinated Gd^{3+}, the magnitude of the effect for a specific cation is anion sensitive. For low charge density anions such as chloride, acetate, bromide, and iodide, there are only slight anion-dependent differences. The overall pattern indicates that, for a given cation, the weakening of the hydrogen bonding within the hydration layer increases with increasing charge density of the anion, as reflected in the progression iodide > bromide > chloride ≫ fluoride. The overall pattern is consistent with the model, to be discussed below, in which the anion effect is modulated by the cation, with the effect being greatest for high charge density cations.

The proposed model is depicted in the Figure 7 schematic that shows key elements that account for the vibronic spectra results. The changes in the OH stretching frequency in the vibronic spectra report on the strength of interaction **H** between the waters in the first hydration layer and the solvent molecules (water or anions) in the second-shell hydration layer. There are three potential influences perturbing interaction **H**: influence 1, due to the cation and its cluster of waters that comprise its hydration shell; influence 2, due to the anion; and influence 3, due to the population of free waters not directly interacting with either the anion or the cation. It has been shown using GVSBS that influence 3 can be modulated with the addition of osmolytes

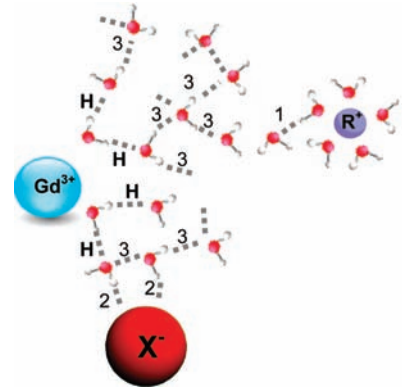

Figure 7. Schematic showing the interactions that affect **H**: the hydrogen bonding between the first and second hydration shell waters around Gd^{3+}. Cation R^+ can exert its effect indirectly either by disrupting nearby water clusters (influence 3), which in turn results in a weakening of the hydrogen bonding between the free waters and the hydration waters of the Gd^{3+}, or by sequestering free waters, thus enhancing anion X^- effects (influence 2). See details in the text.

such as sugars and glycerol that enhance the formation of hydrogen-bonding networks, which in turn increases **H**.[69]

The cation water clusters are expected to have an indirect effect on **H**. This follows because the weakening effect of cations is not likely due to a direct polarity effect between the two positively charged cations that can be expected to be separated by at least several layers of water under the conditions of these measurements.

There are two possible indirect ways that the high charge density cations influence interaction **H**. Both effects arise from

(69) Roche, C. J.; Guo, F.; Friedman, J. M. *J. Biol. Chem.* **2006**, *281*, 38757–38768.

the formation of a tight cluster of waters around the high charge density cation. The first effect is through the cation-induced enhancement in the relative population of high-density water through disruption of hydrogen bonding in the vicinity of the high charge density cation (influence 1). This effect originates from the ordering of water in the hydration shell of the added cations that inhibits the formation of the optimum configuration needed to form low-density water.[7,23] As a consequence, there is a further buildup of the relative concentration of high-density water. The waters participating in a high-density water cluster do not hydrogen bond to the hydration waters as effectively as those in low-density water clusters (influence 3 in the schematic).

The second effect is due to the sequestration of water in the tight hydration shell of the high charge density cations.[70] With increasing sequestration of water, there is a greater probability of an anion participating in the hydrogen-bonding interactions associated with the hydration shell of the Gd^{3+}. The presented results indicate that chloride, bromide, and iodide are not as effective as free (nonsequestered) water with respect to hydrogen binding to the waters in first hydration shell. In contrast, the results are indicative of fluoride ion being able to strongly participate in or enhance, through some indirect mechanism, the hydrogen bonding among hydration layer waters. This difference between anions may arise from several factors, including steric limitations influencing how well different sized anions integrate into the second hydration shell, or a balance between electrostatics and orientation factors.[23]

The above model is further supported by the results from the glassy matrices derived from trehalose. In the glass, the population of waters capable of participating as "normal" solution-phase mobile waters in the hydrogen bonding within the hydration shell of the Gd^{3+} is reduced due to the recruitment of waters into the hydrogen-bonding network of the glass. Under these conditions, the addition of cations that further sequester mobile waters will further deplete the population of waters capable of participating in the normal hydrogen-bonding pattern within the hydration shell of the Gd^{3+}. As a result, the hydrogen bonding between the first- and second-shell solvent molecules has contributions both from waters that can ot adopt the optimal hydrogen-bonding orientations and from the added anions which, in the case of chloride, do not act as an effective replacement for "normal" mobile waters. Magnesium has been shown to be highly effective at sequestering waters (about six waters tightly bound to Mg^{2+}), thereby reducing the relative population of mobile waters.[69,70] The addition of $MgCl_2$ to the glass results in a very substantial weakening of the hydrogen bonding within the hydration shell of the Gd^{3+}. The effect is not seen for NaCl but is also seen for LiCl (not shown), although not to the same extent as with $MgCl_2$. The pattern fits with the model in that increasing charge density enhances the ability of the cation to sequester water and thus decreases the population of mobile waters that can strongly hydrogen bond to other waters. The use of the glass matrix also allows for a much clearer demonstration relative to solution phase that fluoride is effective in enhancing the hydrogen bonding within the hydration shell.

Implications for Protein Stability. The ordering of the Hofmeister series salts with respect to weakening of the hydrogen bonding within the hydration shell of both free and coordinated Gd^{3+} has implications for the effect of these salts on protein properties. It has been argued that osmolytes such as urea can predispose proteins toward unfolding by enhancing the probability that water enters into the hydrophobic protein interior.[71] The presence of internal water has been reported to cause peptide hydrogen bonds to lengthen,[72] a process consistent with a loosening of the structure. The proposed mechanism for this effect is through a shift in the balance between the entropic forces that favor water entering all accessible volumes within the protein and the enthalpic forces due to hydrogen bonding among waters that favor keeping water in the bulk phase.[69] Weakening of the hydrogen bonding among the external waters would enhance the entropically driven occupancy of internal sites within the protein with water molecules. The present results indicate that, for low-density anion salts, cations should increase the probability for water occupancy within the hydrophobic interior to a degree that scales with increasing charge density of the added cation.

The magnitude of the salt-induced weakening can be estimated through the application of the empirical Bauer−Badger rule, which predicts an enthalpy shift of 0.16 kJ/cm^{-1}.[73,74] This relationship results in a 3 kJ/mol decrease in enthalpy for breaking the local hydrogen bonding in the hydration layer of free Gd^{3+} induced by 1 M $MgCl_2$. In a 4 M $MgCl_2$ solution, the estimated decrease in the enthalpy penalty for disrupting the hydration layer water around the metal binding site is 13 kJ/mol. Considering that most globular proteins are marginally stable, with $\Delta G_{\text{folding}} \approx -40$ kJ/mol,[75−79] it is likely that the osmolyte-dependent stability of the hydration shell waters will contribute to conformational properties, as is seen for the osmolyte-induced quaternary structure transition in a dimeric hemoglobin.[80]

Implications for Protein Function and Functionally Important Protein Dynamics. Proteins must be dynamically active to function. There is growing recognition that the wide varieties of dynamics that drive and modulate protein function are highly responsive to the surrounding solvent.[26−28,81,82] The emerging picture is that protein dynamics can be grouped hierarchically on the basis of to which category of solvent motion they are slaved.[27−30,81,82] There are several basic concepts behind the solvent slaving models. First and foremost is the idea that a given protein molecule, even at equilibrium, can access a large number of conformational substates that are energetically

(70) Kiriukhin, M. Y.; Collins, K. D. *Biophys. Chem.* **2002**, *99*, 155–168.
(71) Bennion, B. J.; Daggett, V. *Proc. Natl. Acad. Sci. U.S.A.* **2003**, *100*, 5142–5147.
(72) Fernandez, A.; Scheraga, H. A. *Proc. Natl. Acad. Sci. U.S.A.* **2003**, *100*, 113–118.
(73) Demmel, F.; Doster, W.; Petry, W.; Schulte, A. *Eur. Biophys. J.* **1997**, *26*, 327–335.
(74) Wap, L. Infrared studies of hydrogen bonding in pure liquids and solutions. In *Water—a comprehensive treatise*; Franks, F; Plenum Press: New York, 1973.
(75) Savage, H.; Elliot, C.; Freeman, C.; Finney, J. *J. Chem. Soc., Faraday Trans.* **1993**, *89*, 2609–2617.
(76) Vogl, T.; Jatzke, C.; Hinz, H. J.; Benz, J.; Huber, R. *Biochemistry* **1997**, *36*, 1657–1668.
(77) Ruvinov, S.; Wang, L.; Ruan, B.; Almog, O.; Gilliland, G. L.; Eisenstein, E.; Bryan, P. N. *Biochemistry* **1997**, *36*, 10414–10421.
(78) Privalov, P. L.; Khechinashvili, N. N. *J. Mol. Biol.* **1974**, *86*, 665–684.
(79) Giver, L.; Gershenson, A.; Freskgard, P. O.; Arnold, F. H. *Proc. Natl. Acad. Sci. U.S.A.* **1998**, *95*, 12809–12813.
(80) Royer, W. E., Jr.; Pardanani, A.; Gibson, Q. H.; Peterson, E. S.; Friedman, J. M. *Proc. Natl. Acad. Sci. U.S.A.* **1996**, *93*, 14526–14531.
(81) Fenimore, P. W.; Frauenfelder, H.; McMahon, B. H.; Young, R. D. *Proc. Natl. Acad. Sci. U.S.A.* **2004**, *101*, 14408–14413.
(82) Frauenfelder, H.; Fenimore, P. W.; McMahon, B. H. *Biophys. Chem.* **2002**, *98*, 35–48.

comparable in overall stability.[83,84] These substates differ in the details of side-chain packing and orientation, although the overall global tertiary structure is similar for the members of the distribution. As a result of these differences, the substates can be functionally distinct, with only some fraction of the distribution having measurable rates of reactivity. In the absence of solvent motions, the barrier between substates is very high, and as a consequence there is very slow interconversion among substates, resulting in phenomena such as kinetic hole burning.[85−92] When only a limited set of substates are functionally active, the slow-down of the interconversion of substates will result in a shut-down in activity since the majority of the population will not be able to access the active substate conformations. The solvent slaving concept asserts that solvent motions reduce the enthalpic barrier between substates, allowing a quick entropic search among the many substates for the reactive species. This is the molecular basis for the idea of solvent as a lubricant for protein motions. The solvent-controlled barrier between substates now controls the overall enthalpy for the protein process in question, whereas the rate for the observed functional process also depends upon the duration of the entropic search, i.e., the number of substate transitions needed to access the functionally active species. The present results suggest that Hofmeister osmolytes can control protein reactivity by enhancing the barrier between substates as in the case of sugars, polyols that favor increased hydrogen bonding, or decreasing the barrier by weakening the hydrogen bonding between hydration shell waters using the appropriate salts.

Coordination Weakens Hydrogen Bonding within the Hydration Shell of Gd^{3+}. The initial VSB studies showed that the hydrogen bonding within the hydration shell of Gd^{3+} is stronger than that among waters in the bulk phase.[57,93] The present study shows that coordination to a chelate, a peptide, or a protein causes a weakening of the hydrogen bonding within the hydration shell of the Gd^{3+}. In these cases where the Gd^{3+} is coordinated, the weakening of hydrogen bonding is most plausibly explained in terms of steric factors. The confining environment surrounding the coordinated Gd^{3+} cation likely limits the ability of the hydration shell waters to adopt the geometry among the surrounding waters needed to create the low-density water clusters[36,51,69] that are associated with the strongest hydrogen bonding. The more constrained the environment, the weaker is the hydrogen-bonding network, as in the case of Gd^{3+} coordinating peptide mSE3. This proposed weakening of the hydrogen-bonding pattern associated with waters in the environment surrounding a first-shell hydration water on a nanoscale rough surface should result in an increase in the relative concentration of high-density water in that hydration layer. It has also been claimed that the equilibrium between the two species of water clusters solvating nonpolar groups is shifted toward the high-density clusters when a polar group dominates, as in the case for calcium binding sites on the surface of proteins.[36,94] Therefore, at least two factors should lead to the weakened hydrogen bonding among waters surrounding the coordinated Gd^{3+}: (1) steric constraints limiting the formation of the hydrogen-bonding network need to form low-density water clusters and (2) polar groups that disrupt already distorted hydrogen bond patterns, which also favors higher density clusters.

Weakening of the hydrogen bonding among hydration shell waters due to steric constraints on the protein surface has implications for the osmolyte effects. If through the steric factors there is an increase in high-density water on the protein surface, then osmolytes such as Mg^{2+} and urea that do not readily integrate into the hydrogen-bonding network of low-density water clusters should have a higher occupancy in the hydration layer *vis à vis* the bulk solvent. Thus, the rough surface of the protein lowers the enthalpic penalty of moving cations such as Mg^{2+} into the hydration layer and raises the enthalpic penalty for osmolytes such as glycerol that participate in hydrogen-bonding networks.[69] This explanation may also contribute to the apparent discrepancy between the Raman signal from the bulk solvent and the local signal from the GVSBLS, in that the effect on water should be enhanced where the local concentration of the cation is enhanced.

Conclusions

The present study supports a mechanism for the Hofmeister ordering of salts based on a disruption of hydrogen bonding among hydration shell waters (but not bulk water). The observation of combined anion- and cation-specific hydration shell effects raises the prospect for a better understanding of how *in vivo* levels of specific osmolytes modulate protein structure and dynamics. Furthermore, these studies provide a basis for manipulation of protein properties through a universal mechanism based on tuning the hydrogen bonding within the hydration shell waters of proteins.

Acknowledgment. This work was supported through funding from National Institutes of Health Grant P01HL071064 and FJC, A Foundation of Philanthropic Funds. The authors acknowledge and thank Professors Barbara Imperiali (MIT) and Karen Allen (Boston University) for the information, advice, and materials they generously provided.

Supporting Information Available: Comparison and data of several Hofmeister series ions-induced OH GVSBLS shifts of free Gd^{3+} or Gd^{3+} coordinated to calmodulin or mSE3; affinity of calmodulin or SE2/mSE3 peptides for cations; and SE2/mSE3 peptides sequence.This material is available free of charge via the Internet at http://pubs.acs.org.

JA902240J

(83) Austin, R. H.; Beeson, K.; Eisenstein, L.; Frauenfelder, H.; Gunsalus, I. C.; Marshall, V. P. *Science* **1973**, *181*, 541–543.
(84) Austin, R. H.; Beeson, K. W.; Eisenstein, L.; Frauenfelder, H.; Gunsalus, I. C. *Biochemistry* **1975**, *14*, 5355–5373.
(85) Berendzen, J.; Braunstein, D. *Proc. Natl. Acad. Sci. U.S.A.* **1990**, *87*, 1–5.
(86) Campbell, B. F.; Chance, M. R.; Friedman, J. M. *Science* **1987**, *238*, 373–376.
(87) Chavez, M. D.; Courtney, S. H.; Chance, M. R.; Kiula, D.; Nocek, J.; Hoffman, B. M.; Friedman, J. M.; Ondrias, M. R. *Biochemistry* **1990**, *29*, 4844–4852.
(88) Huang, J.; Ridsdale, A.; Wang, J.; Friedman, J. M. *Biochemistry* **1997**, *36*, 14353–14365.
(89) Levantino, M.; Cupane, A.; Zimanyi, L.; Ormos, P. *Proc. Natl. Acad. Sci. U.S.A.* **2004**, *101*, 14402–14407.
(90) Ormos, P.; Ansari, A.; Braunstein, D.; Cowen, B. R.; Frauenfelder, H.; Hong, M. K.; Iben, I. E.; Sauke, T. B.; Steinbach, P. J.; Young, R. D. *Biophys. J.* **1990**, *57*, 191–199.
(91) Srajer, V.; Champion, P. M. *Biochemistry* **1991**, *30*, 7390–7402.
(92) Agmon, N. *Biochemistry* **1988**, *27*, 3507–3511.
(93) Librizzi, F.; Vitrano, E.; Cordone, L. *Biophys. J.* **1999**, *76*, 2727–2734.
(94) Nakasako, M. *Philos. Trans. R. Soc. London B: Biol. Sci.* **2004**, *359*, 1191–1204 (discussion 1204-6).